

Development

Morphological and Phagocytic Profile of Microglia in the Developing Rat Cerebellum^{1,2,3}

 Miguel Perez-Pouchoulen,¹ Jonathan W. VanRyzin,^{1,2} and Margaret M. McCarthy^{1,2}

DOI:<http://dx.doi.org/10.1523/ENEURO.0036-15.2015>

¹Department of Pharmacology, University of Maryland School of Medicine, Baltimore, Maryland 21201, and ²Program in Neuroscience, University of Maryland School of Medicine, Baltimore, Maryland 21201

Abstract

Microglia are being increasingly recognized as playing important roles in neurodevelopment. The cerebellum matures postnatally, undergoing major growth, but the role of microglia in the developing cerebellum is not well understood. Using the laboratory rat we quantified and morphologically categorized microglia throughout the vermis and across development using a design-based unbiased stereology method. We found that microglial morphology changed from amoeboid to ramified during the first 3 postnatal weeks in a region specific manner. These morphological changes were accompanied by the sudden appearance of phagocytic cups during the third postnatal week from P17 to P19, with an approximately fourfold increase compared with the first week, followed by a prompt decline at the end of the third week. The microglial phagocytic cups were significantly higher in the granular layer (~69%) than in the molecular layer (ML; ~31%) during a 3 d window, and present on ~67% of microglia with thick processes and ~33% of microglia with thin processes. Similar proportions of phagocytic cups associated to microglia with either thick or thin processes were found in the ML. We observed cell nuclei fragmentation and cleaved caspase-3 expression within some microglial phagocytic cups, presumably from dying granule neurons. At P17 males showed an approximately twofold increase in microglia with thin processes compared with females. Our findings indicate a continuous process of microglial maturation and a nonuniform distribution of microglia in the cerebellar cortex that implicates microglia as an important cellular component of the developing cerebellum.

Key words: cell death; development; microglia; phagocytosis; sex difference; vermis

Significance Statement

Microglia are the resident immune cells of the brain and constantly survey their local environment in order to eliminate cellular debris after injury or infection. During brain development, microglia participate in neurite growth, synaptic pruning, and apoptosis, all of which are essential processes to the establishment of neuronal circuits. The cerebellum undergoes major growth and synaptic reorganization after birth, leading to the development of cerebellar circuits which are involved in motor and cognitive functions. The role of microglia in the developing cerebellum is not well understood. This study provides important foundational profiles of microglial development in the cerebellum, a vulnerable structure to alteration during development, and contributes to the growing appreciation of the clearance activity of microglia during postnatal development.

Introduction

Microglia are the resident macrophages of the CNS and play important roles during both normal functioning and in disease or injury. Microglia exhibit diverse morphological features across the CNS and phases of the lifespan (Tremblay et al., 2011). In the adult brain, microglia are known to actively survey their environment through their ramified processes and they dramatically change their morphology in response to damage or infection in order to repair the CNS (Ayoub and Salm, 2003; Nimmerjahn et al., 2005; Ransohoff and Perry, 2009; Nayak et al., 2014). These morphological changes are accompanied by phagocytosis to remove dead cells or cellular debris (Vargas et al., 2005; Cătălin et al., 2013), giving microglia the title of the scavengers of the CNS. Recent evidence suggests microglia are involved in normal development of the brain including neurite growth, synaptic pruning, spinogenesis, and apoptosis (Marín-Teva et al., 2004; Paolicelli et al., 2011; Schafer et al., 2012; Lenz et al., 2013; Kaur et al., 2014). During development microglia undergo morphological changes in both cell body and configuration of their processes, changing from round to ramified, with intermediate stages as the brain matures (Wu et al., 1992; Schwarz et al., 2012). Thus, microglia have important functions impacting the development and formation of neural circuits in the CNS. What is not well understood is whether these functions occur according to a developmental timeframe and how they might differ between brain regions.

The cerebellum is a brain structure involved in many functions including motor control and coordination (Glickstein, 1992; Glickstein et al., 2009), as well as nonmotor functions, such as attention, working memory, language, nociception, pain, addiction, and reward (Rapoport et al., 2000; Gottwald et al., 2003; Holstege et al., 2003; Saab and Willis, 2003; Miquel et al., 2009; Strick et al., 2009; Durisko and Fiez, 2010; Moulton et al., 2010, 2014; Murdoch, 2010; Strata, 2015). The anatomy of the cerebellum consists of an organized and uniform cytoarchitecture that allows systematic and efficient communication among the cerebellar neurons (Voogd and Glickstein, 1998; Sillitoe and Joyner, 2007; Apps and Hawkes, 2009). The human cerebellum matures postnatally and under-

goes major growth and neuronal reorganization during the first 2 years after birth (Abraham et al., 2001; ten Donkelaar et al., 2003; Butts et al., 2014). In rats, cerebellar maturation occurs during the first 3 postnatal weeks with dramatic anatomical changes involving an increase in both cell density and mass volume (Heinsen, 1977; Altman, 1982; Goldowitz and Hamre, 1998). The cerebellar cortex consists of three anatomical layers containing different types of neurons with distinct timeframes of maturation. Maturation of the cerebellar circuitry involves the production and removal of cells, as well as spinogenesis and synaptogenesis, among others (Altman, 1972; Wood et al., 1993; Sarna and Hawkes, 2003; Tanaka, 2009; Haraguchi et al., 2012). Microglia regulate synapses in the developing brain in areas, such as the visual cortex, hippocampus, and retinogeniculate system (Tremblay et al., 2010; Paolicelli et al., 2011; Schafer et al., 2012). However, the number of studies on the role of microglia during postnatal development remain relatively low. In the cerebellum microglia are distributed in both gray and white matter throughout the lifespan across diverse species, and there is a distinct arrangement of microglia processes according to location in the cerebellar cortex (Ashwell, 1990; Vela et al., 1995; Cuadros et al., 1997). Microglia can induce apoptosis of Purkinje neurons *in vitro* (Marín-Teva et al., 2004), but this is not established *in vivo* under normal conditions and overall the role of microglia during postnatal development of the cerebellum is not well understood.

The overarching goal of this report is to profile anatomical changes of microglia during postnatal development of the cerebellum. We hypothesized microglia change their morphological profile and cell density in direct relationship to the maturation of the cerebellum, as well as the anatomical location within the cerebellar cortex. Thus, the purpose of the current study was twofold: first, to identify the morphological profile of microglia across the postnatal developing cerebellum using the ionized calcium-binding adapter molecule 1 (Iba1), which is a microglia marker (Ito et al., 1998); and second, to determine whether the morphological profile of microglia, as well as their phagocytic capability, differ according to location in the cerebellar cortex.

Materials and Methods

Animals

Timed pregnant Sprague-Dawley rats purchased from Charles River Laboratories or raised in our breeding colony were allowed to deliver naturally under standard laboratory conditions. Male and female rat pups were used and the day of birth was denoted as postnatal day (P) 0. All animals were housed in polycarbonate cages (20 × 40 × 20 cm) with corncob bedding under 12 h reverse light/dark cycle, with *ad libitum* water and food. All animal procedures were performed in accordance with the University of Maryland animal care and use committee's regulations.

Received April 21, 2015; accepted August 12, 2015; First published August 18, 2015.

¹The authors declare no competing financial interests.

²Author contributions: M.P.P. and M.M.M. designed research; M.P.P. performed research; J.W.V. and M.M.M. contributed unpublished reagents/analytic tools; M.P.P. analyzed data; M.P.P. and M.M.M. wrote the paper.

³This work was supported by the NIH Grant R01-MH091424 to M.M.M. and CONACYT (Consejo Nacional de Ciencia y Tecnología, Mexico) Postdoctoral Fellowship 236296 to M.P.P.

Correspondence should be addressed to Dr Miguel Perez-Pouchoulen and Dr Margaret M. McCarthy, 655 West Baltimore Street, BRB-5-014, Baltimore, MD 21201. E-mails: mpouchoulen@som.umaryland.edu and mmccarthy@som.umaryland.edu.

DOI: <http://dx.doi.org/10.1523/ENEURO.0036-15.2015>

Copyright © 2015 Perez-Pouchoulen et al.

This is an open-access article distributed under the terms of the Creative Commons Attribution 4.0 International, which permits unrestricted use, distribution and reproduction in any medium provided that the original work is properly attributed.

Immunohistochemistry

Animals were deeply anesthetized with Fatal Plus (Vortech Pharmaceuticals) and transcardially perfused with 0.9% saline solution followed by 4% paraformaldehyde. The entire cerebellums were removed and postfixed overnight in 4% paraformaldehyde, and cryoprotected with 30% sucrose until they were saturated. The cerebellums were sagittally sectioned on a cryostat at a thickness of 45 μm . Free-floating cerebellar slices from different time points between P5 and P21 were rinsed with 0.1 M phosphate buffered saline (PBS), incubated with 3% hydrogen peroxide in PBS for 30 min, and then rinsed again. Sections were coincubated with a polyclonal antibody against Iba1 (1:10000, Wako Chemicals), a microglia marker (Ito et al., 1998), in 10% of bovine serum albumin (BSA) in PBS with 0.4% Triton X-100 (PBS-T) for 30 min at room temperature (RT) with constant agitation, then kept for 24 h at 4°C with constant agitation. Subsequently, sections were rinsed in PBS and incubated with biotinylated anti-rabbit secondary (1:500, Vector Laboratories) in 0.4% PBS-T for 1 h at RT followed by rinses in PBS. Sections were incubated with ABC complex (1:500, Vector Laboratories) in 0.4% PBS-T for 1 h at RT. Iba1-positive cells were visualized using nickel-enhanced diaminobenzidine (Sigma-Aldrich D-5905) as chromogen for 8–10 min incubation at which point sections displayed a dark purple staining. Finally, sections were exhaustively rinsed in PBS, mounted on silane-coated slides, cleared with ascending alcohol concentrations, defatted with xylene, and coverslipped with DPX mounting medium.

Fluorescence immunohistochemistry

In order to colocalize microglial phagocytic cups and fragmented nuclei, Iba1 and DAPI were used, respectively. Free-floating tissue sections from P17 cerebellums were rinsed with 0.1 M PBS, incubated with 3% hydrogen peroxide in PBS for 30 min, rinsed, and then incubated with 0.3 M glycine in 0.4% PBS-T for 60 min. Subsequently, sections were incubated with Iba1 (1:1000, Wako Chemicals) in 0.4% PBS-T containing 10% BSA for 30 min at RT with constant agitation, and then kept for 24 h at 4°C with constant agitation. After primary incubation, sections were rinsed in PBS and incubated with the secondary antibody anti-rabbit AlexaFluor 594 (1:500; Invitrogen) in PBS-T for 120 min in the dark. Sections were then rinsed, mounted and cover-slipped using Hardset mounting medium containing DAPI (Vector Laboratories).

To colocalize dead or dying cells with microglial phagocytic cups, we followed the fluorescence protocol described above to identify the cellular death marker cleaved caspase-3 (1:750, Cell Signaling Technology) and Iba1 (1:1000, Abcam) on P17 cerebellar sections (both cleaved caspase-3 and Iba1 antibodies were incubated together). Anti-rabbit AlexaFluor 488 (1:500; Invitrogen) and anti-goat AlexaFluor 594 (1:500, Invitrogen) were used as secondary antibodies.

Nissl staining

Sagittal sections (45 μm) from P5, P7, P14, P17, and P21 vermis were stained with cresyl violet in order to identify pyknotic bodies. Cerebellar sections were

washed with PBS 0.1 M, mounted and dried for 24 h. Subsequently, sections were hydrated with a series of decreasing concentrations of ethanol (95, 70, and 50%) for 2 min followed by two washes of distilled water (dH_2O) for 1 min. After a 30 sec incubation in 0.1% cresyl violet, sections were washed with dH_2O for 1 min and, then incubated in 70% ethanol for 2 min before the differentiation step in 5% alcohol acid (95% ethanol + 5% acetic acid) for 5 min. Sections were then dehydrated with two washes of 95% ethanol for 2 and 1 min, respectively, and a final incubation in xylene for 3 min before cover-slipping with DPX.

Stereological counts

A design-based unbiased stereological method was performed to quantify microglia, phagocytic cups, and pyknotic bodies across the midvermis. We used StereoInvestigator 10 software (Microbrightfield) interfaced with a Nikon Eclipse 80i microscope and an MBF Bioscience 01-MBF-2000R-F-CLR-12 Digital Camera (Color 12 BIT). Six counting regions (cerebellar lobules 1, 3, 5, 6, 8, and 10; Fig. 1A) from every cerebellar section were used for analysis, which are representative of the anterior, posterior, dorsal, and ventral regions of the vermis. A total of four cerebellar sections per animal were used with a physical distance of 225 μm between them. Considering the small size of microglial cells, it is unlikely that any cell was counted twice during the stereological analysis. The optical fractionator probe method was used to estimate cell, phagocytic cup, and pyknotic body densities using a $100 \times 100 \mu\text{m}$ counting frame sampling every 200 μm . We set an optical dissector height of 15 μm with a 2 μm guard zone (top and bottom) to account any change in section thickness during the staining procedure. Both Iba1⁺ cells and phagocytic cups were counted at 20 \times magnification, and pyknotic bodies counts and the diameter of phagocytic cups at 40 \times magnification. All quantifications were carried out under blinded experimental conditions. The overall estimated volume of each counting region sampled in the vermis was used to normalize estimated counts to obtain an estimation of the average density of objects of interest (e.g., microglia, phagocytic cups, pyknotic bodies), which was expressed as an estimated number/ μm^3 (relative density measurement). Although perivascular macrophages are also positive for Iba1, they represent ~4% of the Iba1⁺ population in the brain (Williamson et al., 2011), suggesting a negligible impact of this factor on the data analysis.

Developmental profile of microglia and phagocytic cups

Microglia counts were performed on P5, P7, P10, P12, P14, P17, and P21 cerebellums from intact male and female rat pups ($n = 4$, 2 males + 2 females for each group). Microglia were morphologically characterized based on Lenz et al. (2013) with modifications into four categories; (1) round/amoeboid microglia, (2) stout microglia, (3) microglia with thick processes (short or long), and (4) microglia with thin processes (short or long), as also

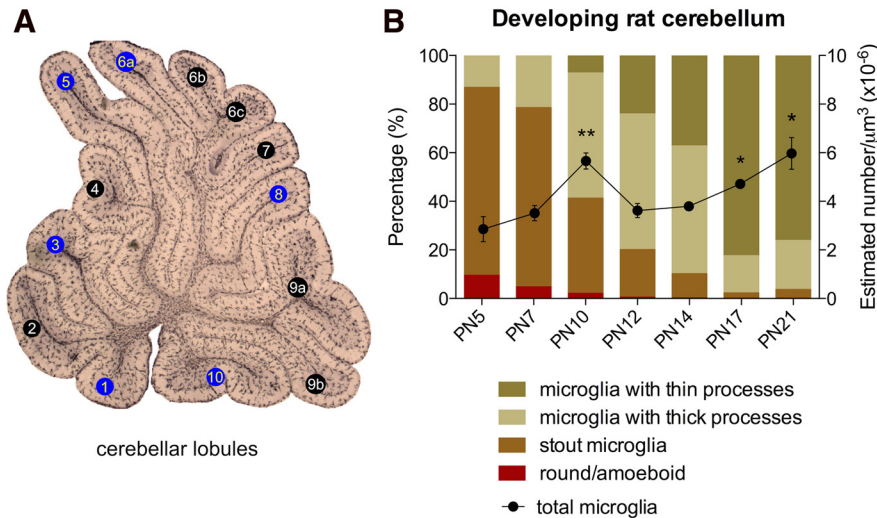


Figure 1. Postnatal microglia across the developing cerebellum. **A**, A sagittal view of the vermis showing the six lobules used to count microglia (blue background). **B**, The density of total microglia significantly increased by 1.58-fold in the third postnatal week compared with the first week ($*p < 0.05$, $**p \leq 0.01$ compared with P5; data are expressed as mean \pm SEM; $n = 4$, 2 males + 2 females for each group). Colored bars depict the proportion of microglia according to morphology at different time points during postnatal development: round/amoeboid microglia are present but infrequent during the first 10 postnatal days while stout microglia are strongly predominant during the first postnatal week, and microglia with both thick and thin processes are more abundant during the second and third week, respectively.

described by others (Wu et al., 1992; Gómez-Gonzalez and Escobar, 2010; Schwarz et al., 2012). For descriptive purposes we identified microglia with thick and thin processes as follows: microglia with thick processes are large cells with an amorphous cell body and with at least two ramified short, long, or both thick processes. Microglia with thin processes are large or small cells with a round and small cell body, with at least four ramified short, long, or both thin processes (more ramified than microglia with thick processes). The density of total microglia, i.e., regardless of morphology, was obtained by summing all four microglial morphologies described above. In addition, cup-shaped invaginations of the plasma membrane formed around cellular debris, infectious agents or dead cells, and called “phagocytic cups” (Swanson, 2008) were also counted in the same cerebellar sections stained with Iba1. To have a clear identification of phagocytic cups, only those located at the tip of microglia processes with a round morphology were counted (Fig. 3B,C). All counts were performed solely in the cerebellar cortex; the white matter was not included. Cellular layers (granular versus molecular) were not distinguished in this experiment, as they are not fully formed at the younger ages.

Quantification of microglia and phagocytic cups in the GL and ML

In a separate cohort of animals, microglia and phagocytic cup counts were performed in the granular layer (GL) and the molecular layer (ML) of the cerebellar cortex on P12, P14, P17, and P21 male and female rat pups ($n = 6$, 3 males + 3 females for each group). At these ages both the GL and ML are well developed. Microglia were categorized based on their morphological features as described

above and the density of total microglia was also obtained.

Quantification of phagocytic cups during the third postnatal week of development

In a third animal cohort aged P15, P16, P17, P18, and P19 ($n = 3$ males + 3 females for each group) the phagocytic cups were counted in both the GL and ML. The morphology of microglia associated with the phagocytic cups was also quantified.

Quantification of pyknotic bodies

Pyknotic bodies were identified using the cresyl violet staining method on *P5, ^P7, *P14, *P17, and *P21 (* $n = 6$, 3 males + 3 females; ^ $n = 4$, 2 males + 2 females). Pyknotic cell quantification was performed using sections from the cerebellar tissues used in the “developmental profile of microglia and phagocytic cups” experiment and followed the same stereological parameters as described above. Likewise, stereological counting was performed in both the GL and ML of the cerebellar cortex.

Phagocytic cup size

The size of microglia phagocytic cups located in both the GL and ML were measured using the quick circle tool on StereoInvestigator 10 (same microscope and camera specifications described above). The same cerebellar regions (cerebellar lobules) used for stereological counts and four cerebellar slices previously stained for Iba1 from ^P10, *P14, *P17, and *P21 cerebellums (^ $n = 4$, 2 males + 2 females; * $n = 8$, 4 males + 4 females) were used in this assay. This analysis was performed on 16 phagocytic cups per animal, which was then averaged for a single measure per animal.

Table 1. Summary of statistical analysis*

Statistical table	Data structure	Type of test	Test value	Effect size	Power
a	Normally distributed	One-way ANOVA	$F_{(6, 21)} = 9.559$	$\eta = 0.73$	0.73
b	Normally distributed	One-way ANOVA	$F_{(6, 21)} = 8.895$	$\eta = 0.72$	0.99
c	Normally distributed	One-way ANOVA	$F_{(6, 21)} = 41.022$	$\eta = 0.92$	1.00
d	Normally distributed	One-way ANOVA	$F_{(6, 21)} = 14.074$	$\eta = 0.80$	1.00
e	Normally distributed	One-way ANOVA	$F_{(6, 21)} = 93.160$	$\eta = 0.96$	1.00
f	Normally distributed	One-way ANOVA	$F_{(6, 21)} = 136.664$	$\eta = 0.97$	1.00
g	Normally distributed	Two-way ANOVA	$F_{(3, 48)} = 9.667$	$\eta = 0.42$	0.99
h	Normally distributed	Two-way ANOVA	$F_{(3, 48)} = 0.418$	—	0.13
i	Normally distributed	Two-way ANOVA	$F_{(3, 48)} = 2.84$	$\eta = 0.18$	0.64
j	Normally distributed	Two-way ANOVA	$F_{(3, 48)} = 0.221$	—	0.09
k	Normally distributed	Two-way ANOVA	$F_{(3, 48)} = 10.517$	$\eta = 0.44$	0.99
l	Normally distributed	Two-way ANOVA	$F_{(3, 48)} = 30.770$	$\eta = 0.69$	1.00
m	Normally distributed	Two-way ANOVA	$F_{(3, 48)} = 5.521$	$\eta = 0.31$	0.97
n	Normally distributed	Two-way ANOVA	$F_{(3, 48)} = 18.271$	$\eta = 0.53$	1.00
o	Normally distributed	Two-way ANOVA	$F_{(3, 48)} = 2.860$	—	0.38
p	Normally distributed	Two-way ANOVA	$F_{(3, 48)} = 54.600$	$\eta = 0.83$	1.00
q	—	—	—	—	—
r	t distribution	Student's t test	$t_{(4)} = 1.278$	—	0.17
s	t distribution	Student's t test	$t_{(4)} = 1.920$	—	0.48
t	t distribution	Student's t test	$t_{(4)} = 3.445$	$d = 3.445$	0.73
u	t distribution	Student's t test	$t_{(4)} = 1.000$	—	0.12
v	t distribution	Student's t test	$t_{(4)} = 0.496$	—	0.1
w	t distribution	Student's t test	$t_{(4)} = 1.683$	—	0.26
x	t distribution	Student's t test	$t_{(4)} = 1.858$	—	0.30
y	t distribution	Student's t test	$t_{(4)} = 1.044$	—	0.13
z	t distribution	Student's t test	$t_{(4)} = 1.726$	—	0.27
aa	t distribution	Student's t test	$t_{(4)} = 0.892$	—	0.11
bb	t distribution	Student's t test	$t_{(4)} = 1.323$	—	0.18

Statistical analysis

All data are expressed as mean \pm SEM and effect size estimate calculations (η and d) reported in Tables 1 and 2. Developmental profile of microglia and phagocytic cup datasets were analyzed using a one-way ANOVA with age as fixed factor. Datasets from microglia and phagocytic cup counts in the GL and ML, phagocytic cup counts during the third postnatal week of development, Nissl staining and pyknotic bodies counts and phagocytic cup size measurement were analyzed using a two-way ANOVA with age and cerebellar layer as fixed factors. All statistical analysis followed a *post hoc* pairwise comparison using the Holm's sequential Bonferroni correction to control for familywise error. Sex differences were studied in the microglia and phagocytic cup counts in the GL and ML dataset only at P17 using a Student's t test for each dependent variable. A summary of statistical analysis performed is reported in Table 1 and pairwise comparisons in Table 2. Significance was denoted when $p \leq 0.05$. All statistical tests were computed in SPSS 22 and graphed using GraphPad Prism 6.

Results

Microglia increase during the first 3 postnatal weeks of development in an age-specific manner

The density of total microglia significantly increased during postnatal development ($p < 0.000$; Fig. 1B; Table 1a). A significant increase in total microglia, compared with P5, was found at P10 ($p = 0.004$), P17 ($p = 0.012$), and P21 ($p = 0.010$), but not at P7 ($p = 0.322$), P12 ($p =$

0.249), or P14 ($p = 0.125$). In addition, the proportion of microglia found in each morphological category changed as the cerebellum developed postnatally. Whereas the proportion of stout microglia were more predominant between P5–P7, the proportion of microglia with both thick and thin processes were more abundant between P10–P14 and P17–P21, respectively (Fig. 1B).

Amoeboid and stout microglia decrease, whereas microglia with both thick and thin processes increase as the cerebellum matures

We categorized and counted microglia based on their morphological features across the vermis at different time points during postnatal development. The density of amoeboid microglia were the least common and they significantly decreased after the first postnatal week ($p < 0.000$)^b. Compared with P5, there were significantly fewer amoeboid microglia at later ages from P10 to P21 (P10, $p = 0.04$; P12, $p = 0.009$; P14, $p = 0.007$; P17, $p = 0.007$; P21, $p = 0.007$; except at P7, $p = 0.232$; Fig. 2A). Likewise, the density of stout microglia decreased after the first postnatal week ($p < 0.000$)^c from P12 to P21 compared with P5 (P12, $p = 0.001$; P14, $p < 0.000$; P17, $p < 0.000$; P21, $p < 0.000$; but not at P7, $p = 0.706$ or P10, $p = 0.108$; Fig. 2B). In contrast, the density of microglia with thick processes significantly increased after the first week ($p < 0.000$)^d with there being more on P7 ($p = 0.038$), P10 ($p < 0.000$), P12 ($p < 0.000$), and P14 ($p = 0.002$) compared with P5. However, by the third postnatal week (*P17 and ^P21) the density of thick

Table 2. Summary of pair comparison tests*

Developmental profile of microglia and phagocytic cups			P7	P10	P12	P14	P17	P21
a	Total microglia	compared with P5	$t_{(6)} = 4.534$	$t_{(6)} = 4.534$ $d = 3.70$	$t_{(6)} = 1.277$	$t_{(6)} = 1.782$	$t_{(6)} = 4.534$ $d = 3.70$	$t_{(6)} = 4.534$ $d = 3.70$
b	Amoeboid microglia	compared with P5	$t_{(6)} = 1.330$	$t_{(6)} = 2.621$ $d = 2.14$	$t_{(6)} = 3.845$ $d = 3.13$	$t_{(6)} = 4.045$ $d = 3.30$	$t_{(6)} = 4.043$ $d = 3.30$	$t_{(6)} = 4.044$ $d = 3.30$
c	Stout microglia	compared with P5	$t_{(6)} = 0.395$	$t_{(6)} = 1.886$	$t_{(6)} = 6.416$ $d = 5.23$	$t_{(6)} = 7.634$ $d = 6.23$	$t_{(6)} = 8.654$ $d = 7.06$	$t_{(6)} = 8.373$ $d = 6.83$
d	Microglia with thick processes	compared with P5	$t_{(6)} = 2.659$ $d = 2.17$	$t_{(6)} = 7.858$ $d = 6.41$	$t_{(6)} = 8.657$ $d = 7.06$	$t_{(6)} = 5.344$ $d = 4.36$	$t_{(6)} = 1.926$	$t_{(6)} = 1.574$
e	Microglia with thin processes	compared with P5	$t_{(6)} = 1.000$	$t_{(6)} = 5.078$ $d = 4.14$	$t_{(6)} = 3.352$ $d = 2.73$	$t_{(6)} = 4.653$ $d = 3.79$	$t_{(6)} = 25.466$ $d = 20.79$	$t_{(6)} = 31.079$ $d = 25.37$
f	Phagocytic cup	compared with P17	P5 $t_{(6)} = 29.336$ $d = 23.95$	P7 $t_{(6)} = 26.068$ $d = 21.28$	P10 $t_{(6)} = 24.687$ $d = 20.15$	P12 $t_{(6)} = 20.255$ $d = 16.53$	P14 $t_{(6)} = 11.571$ $d = 9.44$	P21 $t_{(6)} = 15.762$ $d = 12.86$
Microglia and phagocytic cups in the ML and GL during postnatal development								
g	Total microglia	compared with ML	GL $t_{(10)} = 3.356$ $d = 2.12$	GL $t_{(10)} = 2.640$ $d = 1.66$	GL $t_{(10)} = 3.160$ $d = 1.99$	GL $t_{(10)} = 7.438$ $d = 4.70$		
h	Amoeboid microglia	compared with ML	GL $t_{(10)} = 1.226$	GL $t_{(10)} = 0.049$	GL $t_{(10)} = 1.000$	GL $t_{(10)} = 0.139$		
i	Stoutmicroglia	compared with ML	GL $t_{(10)} = 5.209$ $d = 3.29$	GL $t_{(10)} = 1.192$	GL $t_{(10)} = 3.354$ $d = 2.12$	GL $t_{(10)} = 8.846$ $d = 5.59$		
j	Microglia with thick processes	compared with ML	GL $t_{(10)} = 1.703$	GL $t_{(10)} = 1.326$	GL $t_{(10)} = 0.601$	GL $t_{(10)} = 1.003$		
k	Microglia with thin processes	compared with ML	GL $t_{(10)} = 0.604$	GL $t_{(10)} = 0.116$	GL $t_{(10)} = 2.191$ $d = 1.38$	GL $t_{(10)} = 6.186$ $d = 3.91$		
l	Phagocytic cup	compared with ML	GL $t_{(10)} = 4.013$ $d = 2.53$	GL $t_{(10)} = 2.400$ $d = 1.51$	GL $t_{(10)} = 6.814$ $d = 4.30$	GL $t_{(10)} = 2.279$ $d = 1.44$		
Microglial phagocytic activity during the third postnatal week of development								
m	Phagocytic cup	compared with GL P17	P15 GL $t_{(10)} = 3.978$ $d = 2.51$	P16 GL $t_{(10)} = 2.198$ $d = 1.39$	P18 GL $t_{(10)} = 0.568$	P19 GL $t_{(10)} = 0.518$		
m	Phagocytic cup	compared with ML P17	ML $t_{(10)} = 1.499$	ML $t_{(10)} = 0.029$	ML $t_{(10)} = 1.300$	ML $t_{(10)} = 2.313$ $d = 1.46$		
m	Phagocytic cup	compared with the ML	P15 GL $t_{(10)} = 0.757$	P16 GL $t_{(10)} = 3.052$ $d = 1.93$	P17 GL $t_{(10)} = 4.091$ $d = 2.58$	P18 GL $t_{(10)} = 7.765$ $d = 4.91$	P19 GL $t_{(10)} = 3.348$ $d = 2.11$	
Phagocytic cup size during the third postnatal week of development								
n	Phagocytic cup	compared with P17	P10 $t_{(10)} = 2.037$ $d = 1.28$	P14 $t_{(14)} = 5.262$ $d = 2.81$	P21 $t_{(14)} = 3.547$ $d = 1.73$			
Pyknotic bodies in the GL than the ML during postnatal development								
p	Pyknotic bodies	compared with GL P7	P5 GL $t_{(8)} = 0.328$	P14 GL $t_{(8)} = 34.179$ $d = 24.16$	P17 GL $t_{(8)} = 25.394$ $d = 17.95$	P21 GL $t_{(8)} = 39.642$ $d = 28.03$		
p	Pyknotic bodies	compared with ML P7	ML $t_{(8)} = 1.401$	ML $t_{(8)} = 0.416$	ML $t_{(8)} = 0.729$	ML $t_{(8)} = 0.939$		
p	Pyknotic bodies	compared with ML	P5 GL $t_{(10)} = 7.163$ $d = 4.53$	P7 GL $t_{(6)} = 19.461$ $d = 15.88$	P14 GL $t_{(10)} = 1.628$	P17 GL $t_{(10)} = 0.100$	P21 GL $t_{(10)} = 1.392$	
Sex differences in microglia morphology on P17 cerebellum								
q/u	Amoeboid microglia	compared with females	GL males $t_{(4)} = 0.000$	ML males $t_{(4)} = 1.000$				
r/v	Stout microglia	compared with females	GL males $t_{(4)} = 1.278$	ML males $t_{(4)} = 0.496$				
s/w	Microglia with thick processes	compared with females	GL males $t_{(4)} = 1.920$	ML males $t_{(4)} = 1.683$				
t/x	Microglia with thin processes	compared with females	GL males $t_{(4)} = 3.445$ $d = 3.445$	ML males $t_{(4)} = 1.858$				
y/z	Phagocytic cup	compared with females	GL males $t_{(4)} = 1.044$	ML males $t_{(4)} = 1.726$				
aa/bb	Total microglia	compared with females	GL males $t_{(4)} = 0.892$	ML males $t_{(4)} = 1.323$				

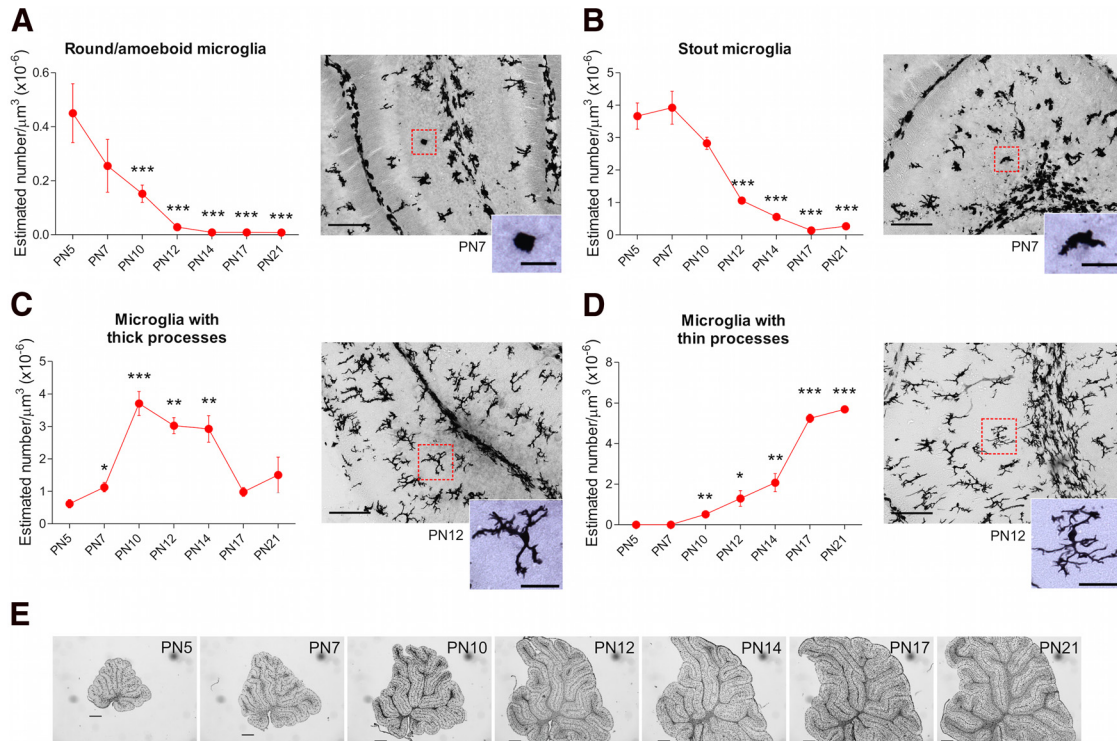


Figure 2. Morphological profile of microglia in the postnatal developing cerebellum. **A**, The frequency of round/amoeboid microglia significantly decreased after the first postnatal week (**B**), as well as stout microglia. **C**, Conversely, the density of microglia with thick processes increased only during the second postnatal week followed by a decrease in the third postnatal week. **D**, The density of microglia with thin processes gradually increased after the first postnatal week doubling their density by the third postnatal week. **E**, Sagittal views of the midvermis, labeled with Iba1, across the first 3 postnatal weeks. All data are expressed as mean \pm SEM ($n = 4$, 2 males + 2 females for each group). Significant differences are denoted by * $p < 0.05$, ** $p < 0.01$, and *** $p < 0.000$ compared with P5. Insets depict a higher magnification of selected microglia (red squares) in each panel. Scale bars: gray scale images, 100 μm ; color images (inset), 25 μm ; **E**, 500 μm (from P5 to P21). Images in **A**, **B**, **C**, and **D** depict the morphology of microglia at two different postnatal ages: P7 (**A**, **B**) and P12 (**C**, **D**).

processed microglia dropped back down to immature levels (* $p = 0.102$ and $\wedge p = 0.167$, respectively; **Fig. 2C**). By contrast, the density of microglia with thin processes steadily increased as the cerebellum developed ($p < 0.000$)^e with a significant difference from P10 until P21 (P10, $p = 0.002$; P12, $p = 0.015$; P14, $p = 0.003$; P17, $p < 0.000$; P21, $p < 0.000$ compared with P5; **Fig. 2D**).

The density of microglia phagocytic cups peaks during the third postnatal week of cerebellar development

The frequency of phagocytic cups changed across development ($p < 0.000$)^f, with the highest density observed on P17 compared with each time point in this experiment (P5, $p < 0.000$; P7, $p < 0.000$; P10, $p < 0.000$; P12, $p < 0.000$; P14, $p < 0.000$; P21, $p < 0.000$; **Fig. 3A**).

There are more microglia in the GL than the ML in the cerebellar cortex

To test whether the density of total microglia and/or their morphology differs based on anatomical location in the cerebellar cortex, we counted microglia separately in both the GL and ML at different time points during postnatal development. A significant interaction for age X cerebellar

layer was found for total microglia ($p < 0.000$)^g. The GL layer had a higher density of total microglia compared with the ML at P12 ($p = 0.007$), P14 ($p = 0.025$), P17 ($p = 0.010$), and P21 ($p < 0.000$; **Fig. 4A**). When we looked at the microglial morphology, there was a significant interaction of age X cerebellar layer for stout microglia ($p = 0.05$)ⁱ. The ML exhibited a higher density of stout microglia than GL at P12 ($p < 0.000$), P17 ($p = 0.007$) and P21 ($p < 0.000$), but not at P14 ($p = 0.261$) (**Fig. 4C**). Likewise, a significant interaction for age X cerebellar layer was detected for microglia with thin processes ($p < 0.000$)^k. We found the GL to have higher density of microglia with thin processes than the ML later in development (P17; $p = 0.05$, P21; $p < 0.000$), but not earlier (P12; $p = 0.56$, P14; $p = 0.91$; **Fig. 4E**). No significant interactions for age X cerebellar layer were found for round/amoeboid microglia ($p = 0.74$; **Fig. 4B**)^h or for microglia with thick processes ($p = 0.88$; **Fig. 4D**)^l.

Phagocytic cups are more frequent in the GL than the ML of the vermis during the third postnatal week

A significant interaction for age X cerebellar layer for phagocytic cups was also found ($p < 0.000$)^l. *Post hoc* pairwise comparison revealed a higher density of phago-

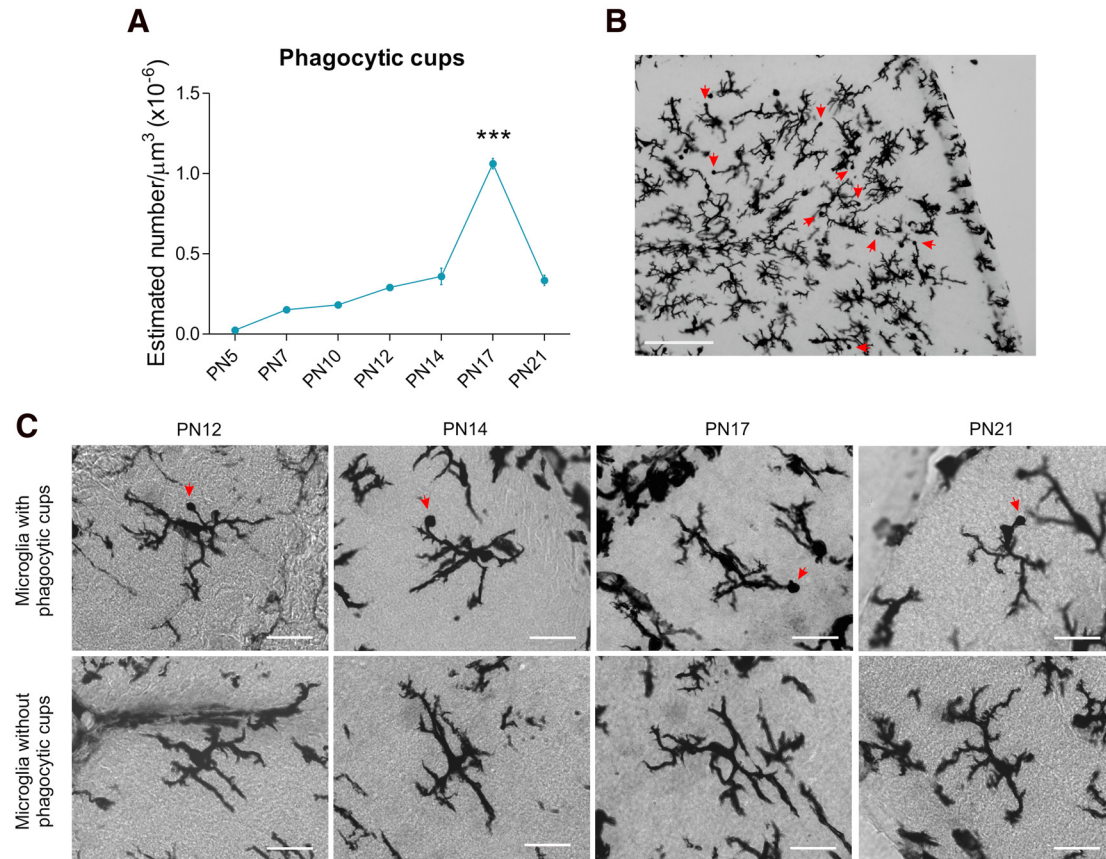


Figure 3. Microglial phagocytosis in the postnatal developing cerebellum. **A**, The highest density of phagocytic cups was observed during the third postnatal week at P17 ($***p < 0.000$ compared with P5, P7, P10, P12, P14, and P21; $n = 4$, 2 males + 2 females for each group). Data are expressed as mean \pm SEM. **B**, Phagocytic cups exhibited by microglia (red arrows) in the developing cerebellum at P17. Scale bar, 100 μm . **C**, Microglia with phagocytic cups (top) or microglia without phagocytic cups (bottom row) at different time points during postnatal development. Scale bars, 25 μm .

cytic cups in the ML than the GL at younger ages (P12, $p = 0.002$; P14, $p = 0.037$). However, this pattern reversed at slightly older ages with the GL exhibiting more phagocytic cups than the ML at P17 ($p < 0.000$) and P21 ($p = 0.046$) (Fig. 5A).

Because phagocytic cups in the developing cerebellum were highest at P17 in the GL (Figs. 3A, 5A), we sought to determine whether this peak was exclusive to that age or more broadly present. Therefore, we counted phagocytic cups on 2 consecutive days before and after P17 in both the ML and the GL of the cerebellar cortex. There was a significant interaction for age \times cerebellar layer in phagocytic cups ($p = 0.001$)^m. *Post hoc* pairwise comparisons revealed the density of phagocytic cups in the GL was lower at P15 ($p = 0.003$) and P16 ($p = 0.05$) compared with P17 (Fig. 5B). No significant differences were found for phagocytic cup density at P18 ($p = 0.583$) or P19 ($p = 0.615$) compared with P17 (Fig. 5B), indicating a plateau from P17 to P19. In contrast, in the ML the density of phagocytic cups significantly decreased at P19 compared with P17 ($p = 0.043$; Fig. 5B). Additionally, we replicated the significant difference between the GL and ML in terms of phagocytic cup density. The GL had a greater density of phagocytic cups than the ML from P16 to P19 (P16,

$p = 0.012$; P17, $p = 0.002$; P18, $p < 0.000$; P19, $p = 0.007$; but not at P15, $p = 0.467$; Fig. 5B).

Additionally, we found the phagocytic cups located in the GL associated exclusively with ramified microglia, with thick and thin processes, from P15 to P19 (Fig. 5C). During this timeframe, the proportion of phagocytic microglia with thick processes ($\geq 68\%$) was higher than the proportion of phagocytic microglia with thin processes ($\geq 16\%$). By P17, the proportion of microglia with thick processes decreased $\sim 16\%$ keeping that proportion until P19. In contrast, the proportion of microglia with thin processes increased $\sim 17\%$ between P15 and P17 maintaining a similar proportion of cells until P19 (Fig. 5C).

Phagocytic cups are largest during the third postnatal week in both the GL and ML

We quantified the size of individual phagocytic cups and a 2×4 ANOVA analysis detected a significant main effect of age ($p < 0.000$)ⁿ. Pairwise comparisons revealed P17 cerebellums have larger phagocytic cups than those found at P10 ($p = 0.06$), P14 ($p < 0.000$), and P21 ($p = 0.003$; Fig. 5D). There was no impact of cerebellar layer on cup size ($p = 0.09$)^o.

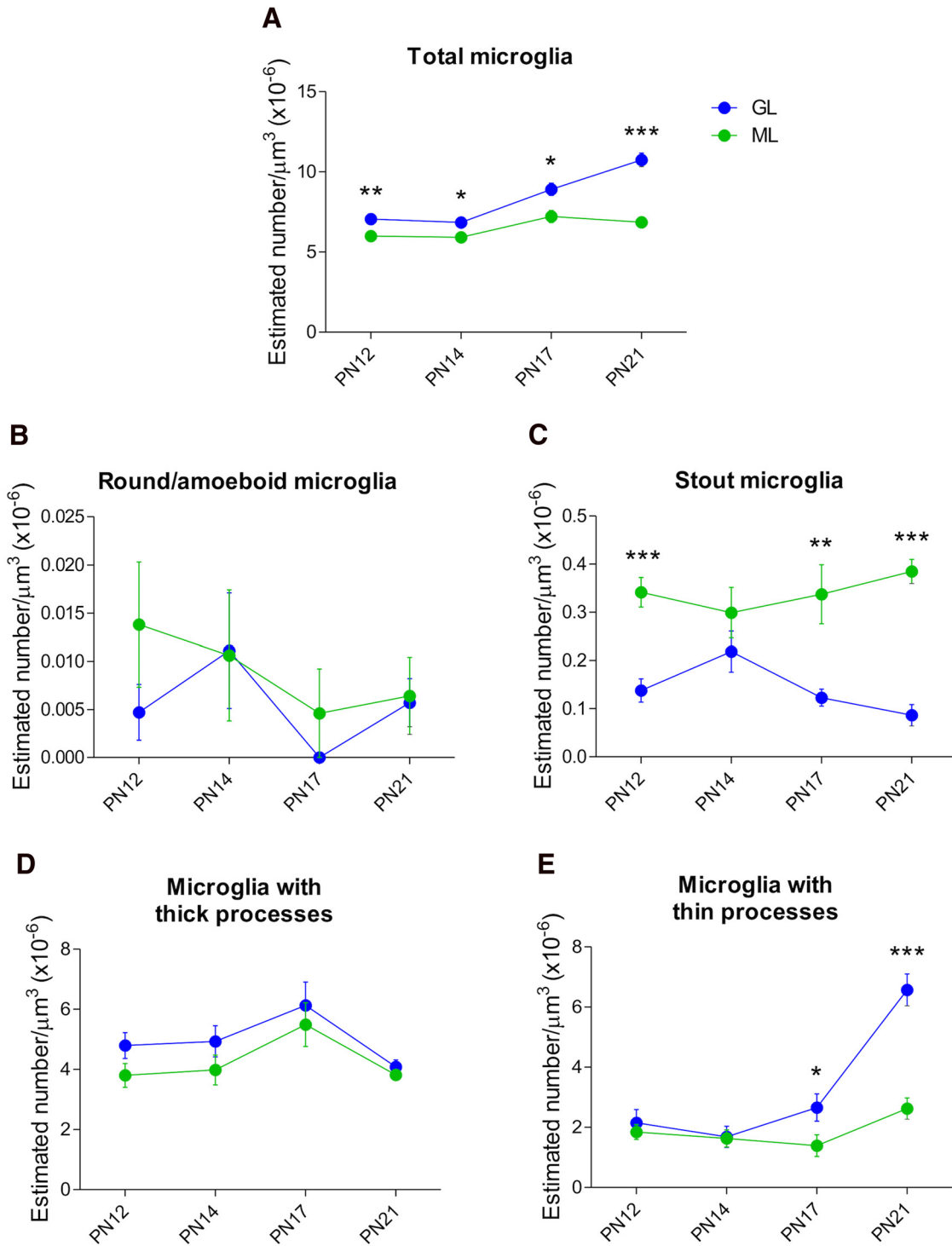


Figure 4. Microglia location in the cerebellar cortex based on morphological classification. **A**, Total microglia were significantly higher in the GL than the ML during the second and third postnatal week in the cerebellum (* $p < 0.05$, ** $p < 0.01$, *** $p < 0.000$). **B**, The density of round/amoeboid microglia was very low and did not differ between the ML and the GL from P12 to P21. **C**, The density of stout microglia was significantly higher in the ML than the GL at all days examined except P14 (** $p < 0.01$, *** $p < 0.000$). **D**, Microglia with thick processes were the most abundant but did not differ between the ML and the GL. **E**, There were significantly more microglia with thin processes in the GL than the ML at P17 and P21 but not at younger ages examined (* $p < 0.05$, *** $p < 0.000$). All data are expressed as mean \pm SEM ($n = 6$, 3 males + 3 females for each group).

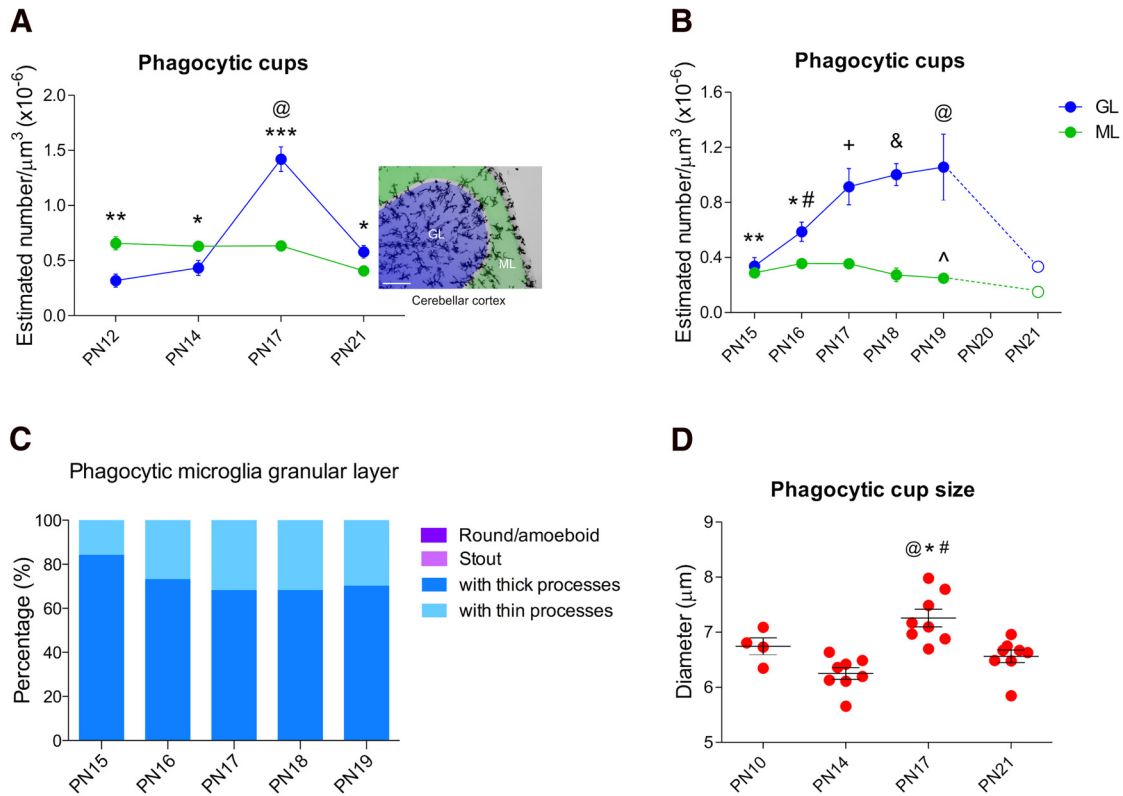


Figure 5. Frequency of phagocytosis by microglia changes by location in the cerebellar cortex across development. **A**, The density of phagocytic cups was higher in the ML than the GL at P12 (** $p < 0.01$), and P14 (* $p < 0.05$), but switched at P17 (***) and P21 (* $p < 0.05$), so that the GL exhibited more phagocytic cups than the ML. The highest density of phagocytic cups was found in the GL at P17 compared with P12, P14, and P21 ($p < 0.000$). Scale bar, 100 μm . **B**, Proportion of microglia that exhibited phagocytic cups in the GL at P17: 67% of all phagocytic microglia had thick processes and 33% had thin processes. No round/amoeboid or stout microglia showed phagocytic cups. **C**, A difference in the density of phagocytic cups was found at younger ages (P15, ** $p = 0.003$; P16, * $p = 0.05$) compared with P17, but no significant differences were found at older ages (P18, $p = 0.583$; P19, $p = 0.615$). In contrast, in the ML, the density of phagocytic cups was lower only at P19 ($p = 0.043$) compared with P17. Additionally, a difference in the density of phagocytic cups between the GL and ML was found from P16 to P19 (P16, # $p < 0.000$; P17, + $p < 0.000$; P18, & $p < 0.000$; P19, @ $p < 0.000$) but not at P15 ($p = 0.467$) ($n = 6$, 3 males + 3 females for each group for **A**, **B**, and **C**). In this experiment the density of phagocytic cups was not counted in animals at P21 but the dashed lines depict the pattern previously observed at the end of the third postnatal week in both the GL and ML (Fig. 5A). **D**, The diameter of microglial phagocytic cups was bigger on P17 compared with P10 (@ $p = 0.06$; see effect size estimation in Table 2), P14 (* $p < 0.000$) and P21 (# $p = 0.003$). All data are expressed as mean \pm SEM ($n = 4$, 2 males + 2 females; * $n = 8$, 4 males + 4 females: ^P10, *P14, *P17, and *P21).

Pyknotic bodies are more prevalent in the GL than the ML only during the first postnatal week

We quantified the density of pyknotic bodies in the cerebellar cortex (Fig. 6B) at different postnatal time points to establish a pattern of cell death and to see whether it correlated with the pattern of increased phagocytosis at P17. A significant interaction between age X cerebellar layer for pyknotic bodies was detected ($p < 0.000$). Pyknotic bodies density decreased in the GL at P14 ($p < 0.000$), P17 ($p < 0.000$) and P21 ($p < 0.000$) compared with P7, but not at P5 ($p = 0.751$; Fig. 6A). No changes in the density of pyknotic bodies were detected in the ML in any of the developmental time points analyzed compared with P7 (P5, $p = 0.199$; P14, $p = 0.688$; P17, $p = 0.487$; P21, $p = 0.375$; Fig. 6). Moreover, there were more pyknotic bodies in the GL than the ML at P5 ($p < 0.000$) and P7 ($p < 0.000$), but not at later ages (P14, $p = 0.134$; P17, $p = 0.922$; P21, $p = 0.194$; Fig. 6A). These data indicate

there is not a clear relationship between the appearance of both phagocytic cups and pyknotic bodies in the developing cerebellum.

We also found colocalization of pyknotic cell bodies within some phagocytic cups in the cerebellar cortex at P17 (Fig. 6C). As expected, the cell death marker cleaved caspase-3 also colocalized with some phagocytic cups at P17 (Fig. 6D). However, we also detected cleaved caspase-3 broadly in the cerebellar cortex and white matter, with an intense expression in the Purkinje cell layer. This did not appear related to cell death (see Discussion).

Males have more microglia with thin processes than females in the GL at P17

We looked at sex differences in the cerebellum in terms of microglia density at P17 in both the GL and ML to determine whether at this unique time point the cerebellum develops differently according to sex. We found that

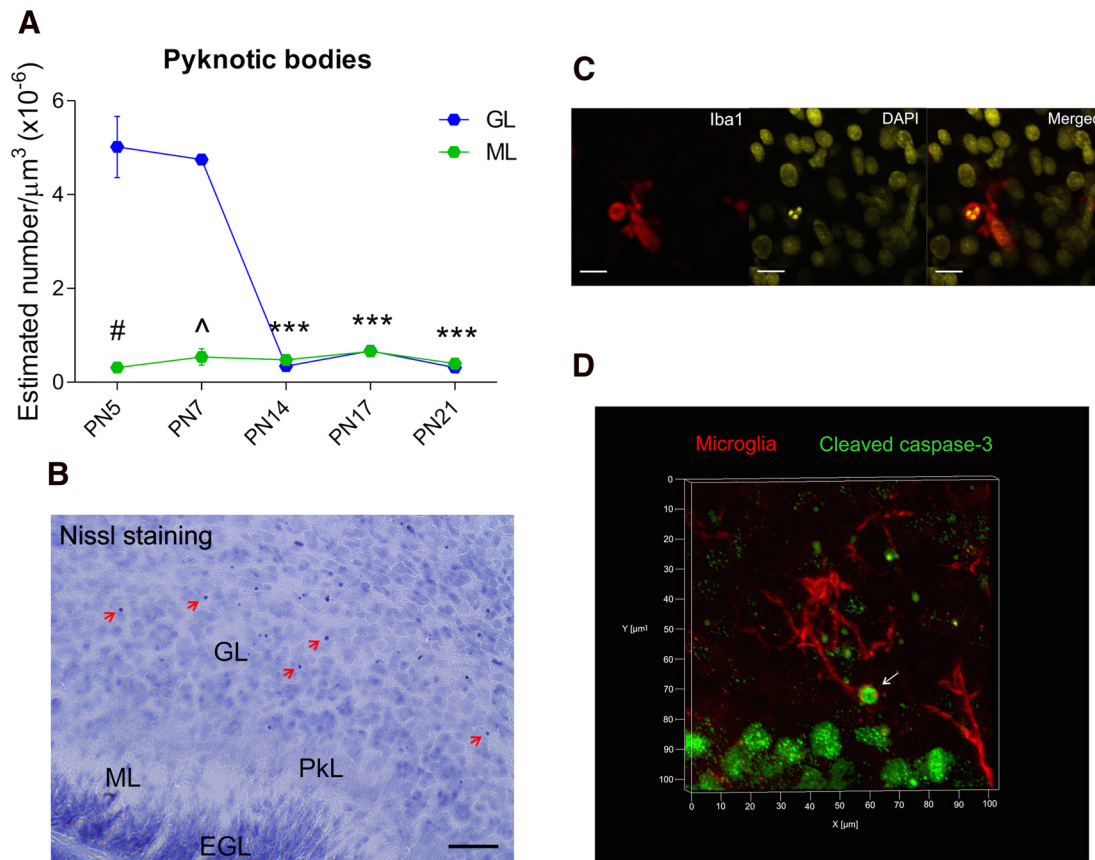


Figure 6. Identification of pyknotic bodies by Nissl staining in the postnatal developing cerebellum. **A**, The density of pyknotic bodies (red arrows) decreased only in the GL after the first postnatal week at P14, P17 and P21 ($***p < 0.000$), but not at P7 ($p = 0.302$), compared with P5. No changes in the density of pyknotic bodies were detected in the ML across the developmental time points analyzed when compared with P7 (P5, $p = 0.199$; P14, $p = 0.688$; P17, $p = 0.487$; P21, $p = 0.375$). The GL exhibited more pyknotic bodies than the ML only during the first postnatal week at P5 ($^{\#}p < 0.000$) and P7 ($^{\wedge}p < 0.000$). Scale bar, 25 μm . Data are expressed as mean \pm SEM ($^*n = 6$, 3 males + 3 females; $^{\wedge}n = 4$, 2 males + 2 females: *P5 , $^{\wedge}P7$, *P14 , *P17 , and *P21). **B**, P7 cerebellar sagittal section stained with cresyl violet showing pyknotic bodies pointed out by red arrows. Pk, Purkinje layer; EGL, external granular layer. **C**, Confocal colocalization of a pyknotic body (fragmented nucleus in yellow) and a phagocytic cup (red) in the cerebellar cortex at P17. Scale bars, 15 μm . **D**, 3D confocal image depicting a colocalization of a microglial phagocytic cup (red) and a cleaved caspase-3-positive cell (green) at the tip of a microglia process (white arrow).

males have a higher density of microglia with thin processes than females in the GL ($p = 0.026^{\text{f}}$; Fig. 7D). No significant differences were found in any other of the morphological categorization of microglia in the GL (round/amoeboid; $t_{(4)} = 0.000^{\text{g}}$; stout, $p = 0.270^{\text{r}}$; with thick processes, $p = 0.127^{\text{s}}$; Fig. 7A–C) or the ML (round/amoeboid, $p = 0.375^{\text{u}}$; stout, $p = 0.646^{\text{v}}$; with thick processes, $p = 0.168^{\text{w}}$; with thin processes, $p = 0.137^{\text{x}}$; Fig. 7E–H). Also, there were no significant differences between males and females for phagocytic cups in the GL ($p = 0.356^{\text{y}}$) or ML ($p = 0.159^{\text{z}}$). The same results were found for total microglia (GL, $p = 0.423^{\text{aa}}$; ML, $p = 0.256^{\text{bb}}$).

Discussion

The rat cerebellum reaches maturation during the first 3 postnatal weeks and undergoes remarkable anatomical changes during this time (Heinsen, 1977; Altman, 1982; Goldowitz and Hamre, 1998; Sotelo, 2004; Sillitoe and

Joyner, 2007; Butts et al., 2014). We found microglia also dramatically change their morphological profile from round to ramified in the cerebellar cortex during this dynamic period of development (Fig. 1B). This developmental profile of microglia in the cerebellum is consistent with previous findings in other regions of the CNS, i.e., going from round to ramified morphology (Wu et al., 1992; Schwarz et al., 2012). However, morphological differences in microglia varied by subregion (ML vs GL), suggesting an important role for local factors in regulating differentiation. A decline in round/amoeboid microglia after the first postnatal week in the entire mouse cerebellum has also been reported, although with a different developmental profile (Ashwell, 1990). The frequency of stout microglia also declined along a similar time course to the amoeboid, whereas microglia with both thick and thin processes increased as the cerebellum matured. These data indicate a continuous process of microglial maturation during the first 3 post-

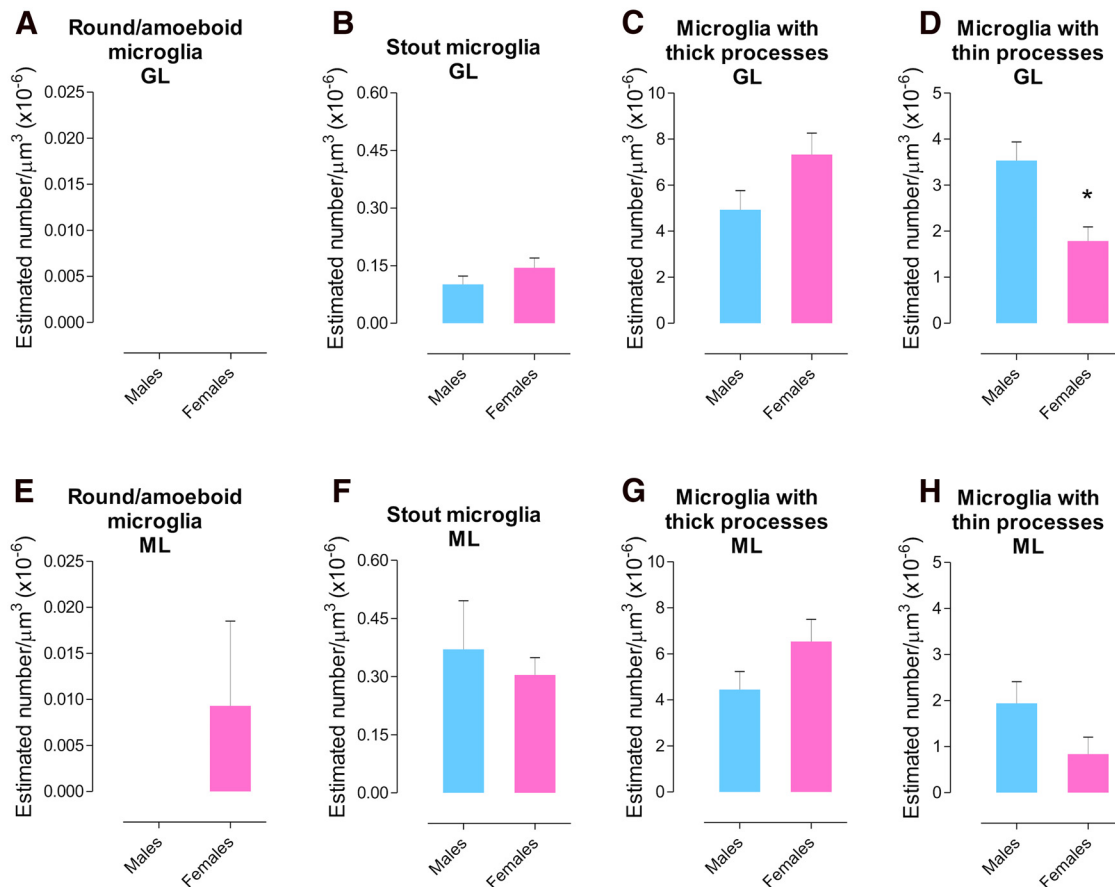


Figure 7. Microglial sex differences in the developing cerebellum. **A–D**, Estimated density of microglia based on morphology in the GL at P17. Males had more microglia with thin processes than females ($p = 0.026$). No significant differences were found for sex in round/amoeboid microglia, stout microglia ($p = 0.270$) or microglia with thick processes ($p = 0.127$). **E–H**, Estimated density of microglia based on morphology in the ML at P17. The statistical analysis indicated no sex differences in round/amoeboid ($p = 0.375$), stout ($p = 0.646$), microglia with thick processes ($p = 0.168$), or microglia with thin processes ($p = 0.137$). Data are expressed as mean \pm SEM ($n = 6$, 3 males + 3 females for each group).

natal weeks that might be related to a specific function as the cerebellum develops including regulation of cell death and synaptic pruning.

Microglia remove apoptotic cellular debris through phagocytosis (Parnaik et al., 2000; Neumann et al., 2009; Sierra et al., 2010, 2013). Phagocytosis by ramified microglia (with thick or thin processes) requires the formation of round structures of actin called phagocytic cups (Swanson, 2008). The appearance of a marked increase in phagocytic cups during the third postnatal week, particularly at P17, suggests this is a critical period for microglial phagocytosis in the developing cerebellum. Moreover, the content of some phagocytic cups indicated pyknotic bodies, suggesting the engulfment of apoptotic cells, as has been observed in other regions of the CNS (Sierra et al., 2010). Previous evidence of microglial phagocytosis in the developing cerebellum focused on round or amoeboid microglia (Ashwell, 1990). Here we show that ramified microglia are the dominant committers of phagocytosis during the second and third postnatal week of development in the cerebellum. However, how

phagocytic microglia contribute to the establishment of the cerebellar circuit remains poorly understood.

The cerebellar cortex is organized into three anatomical layers that contain different types of neurons with specific developmental timeframes and populations (Altman, 1982; Sotelo, 2004). The GL consists of a larger variety and population of cells compared with the ML and the Purkinje layer that only contains two different interneurons and one type of neuron, respectively (Burgoyne and Cambray-Deakin, 1988; Voogd and Glickstein, 1998; Apps and Garwicz, 2005). We observed differences between the GL and ML in terms of microglial population. The overall number of microglia are consistently higher in the GL than the ML from P12 to P21, but interestingly, this pattern changes when the morphology of microglia is taken into account. Although more stout microglia are present in the ML than the GL during the second and third postnatal week, there are more microglia with thin processes in the GL than the ML, but only during the third postnatal week. Stout microglia are still differentiating and changing into the ramified form as part of their maturation

likely in their final location in the cerebellar cortex. On the other hand, microglia with thin processes have already reached their final location in the cerebellar cortex increasing in cell density as the cerebellum matures. Thus, our findings indicate that microglia are not uniformly distributed in the cerebellar cortex of the developing cerebellum, a finding consistent with a previous report in the young (>25 d) and adult mouse cerebellum (>90 d; Vela et al., 1995).

A surprising observation was the high degree of regional and temporal specificity of the phagocytic activity of microglia, an important function for the normal developing brain as well as in the adult brain under infectious or damage situations (Neumann et al., 2009; Sierra et al., 2013). Phagocytosis by microglia was higher in the ML during the second postnatal week but a few days later the GL had dramatically more phagocytic cups until the end of the third week. This switch may be driven by a combination of processes occurring in the GL required for its maturation, such as cell proliferation and formation of synapses (Altman, 1972; Burgoyne and Cambray-Deakin, 1988; Carletti and Rossi, 2008), but also cell death.

We found a peak of phagocytic cups density at P17, which was localized to the GL and persisted for a 3 d window in the third postnatal week of development. During this window the proportion of microglia with thick processes decreased ~16%, whereas the proportion of microglia with thin processes increased ~17%, suggesting a final maturation phase. Although this change is related to maturation of the cerebellum, whether it is critical for the establishment of the GL remains unknown. We found no evidence to suggest the increased phagocytosis at P17 was solely for the removal of dead cells since the pattern of pyknotic bodies, a measure of cell death, bore no resemblance to the pattern of microglial phagocytosis. Similar results in the mouse developing cerebellum are in accordance with ours (Wood et al., 1993; Lossi et al., 2002). Nonetheless, the colocalization of pyknotic bodies and cleaved caspase-3 with some phagocytic cups at P17 in the cerebellar cortex indicates that microglia are removing apoptotic cells. Interestingly, our observation of cleaved caspase-3 expression broadly in the cerebellum suggests it may be participating in nonapoptotic processes, such as cell differentiation, cell proliferation, neurite pruning, and synaptic plasticity as described by others (Oomman et al., 2004; D'Amelio et al., 2012; Hyman and Yuan, 2012; Shalini et al., 2015). The removal of apoptotic cells by ramified microglia is supported by the size of the phagocytic cups, which correlates with the size of granule neurons (Burgoyne and Cambray-Deakin, 1988), the only neurons proliferating during the second and third postnatal weeks in the cerebellum (Carletti and Rossi, 2008). Nevertheless, synaptic and axonal debris could also undergo removal by microglia as part of the synaptic changes and maturation of the climbing and mossy fibers at this age (Goldowitz and Hamre, 1998; Hashimoto and Kano, 2005; McKay and Turner, 2005).

Microglia regulate synapses and axons during development in other regions of the CNS during the second and third postnatal weeks (Berbel and Innocenti, 1988; Tremblay et al., 2010; Paolicelli et al., 2011; Schafer et al., 2012). This implicates microglia as being directly involved in the remodeling of neural synaptic circuits. By the second postnatal week rat pups generally open their eyes (Reiter et al., 1975) and also begin to respond to auditory signals (Friauf, 1992). By the third postnatal week play behavior appears (Meaney and Stewart, 1981; Panksepp, 1981; Auger and Olesen, 2009). Thus, the cerebellum processes motor and sensorial stimulation that may regulate synaptic connections and therefore, the phagocytic activity of microglia.

We measured the size of phagocytic cups and found them to differ according to age, but not to location in the cerebellar cortex. The size of the cups was largest on P17, when phagocytosis peaks in the GL, but not in the ML. This finding suggests that phagocytic microglia are engulfing either larger or greater amounts of cellular debris at P17. The difference between the largest and the smallest phagocytic cup was equal to 1 μm , which might indicate a precise and efficient process of phagocytic cup formation. However, whether this difference carries a significant biological function is not clear.

Evidence in this study supports the conclusion that P17 is an important time point for microglia function in the development of the cerebellum. This function depends on the location of microglia in the cerebellar cortex, but we also found sex to influence microglia in the cerebellum as males showed more microglia with thin processes than females in the GL, but not in the ML, at P17. Microglia with thin processes presumably have reached their final location in the cerebellar cortex; therefore, they are matured and surveying their local environment suggesting a different pattern in microglial maturation in the GL according to sex that might influence the assembly of the cerebellar circuit. However, there was no sex difference in frequency of phagocytic cups in the cerebellar layers at this age, indicating that phagocytosis by microglia is similar between males and females in the developing cerebellum. Sex differences have been reported in both the adult human and rat cerebellums in terms of anatomy and function (Dean and McCarthy, 2008). Here we show a sex difference at the cellular level in a structure vulnerable to damage during development. The cerebellum is commonly altered in developmental disorders, such as autism, a disorder with gender bias in its prevalence (Bauman and Kemper, 2005; Amaral et al., 2008; Perez-Pouchoulen et al., 2012; Werling and Geschwind, 2013). Therefore, these results might give insights to address other ways to explore the developing cerebellum under normal and abnormal conditions.

Altogether, this work contributes to the understanding of the role of microglia in the rat cerebellum during normal development with a particular focus on the development of the vermis, a vulnerable structure to developmental alterations. To understand what is inadequate in the abnormal developing cerebellum we have to understand first

how the cerebellum is formed and the contribution of microglia to this end.

References

- Abraham H, Tornóczy T, Kosztlányi G, Seress L (2001) Cell formation in the cortical layers of the developing human cerebellum. *Int J Dev Neurosci* 19:53–62. [Medline](#)
- Altman J (1972) Postnatal development of the cerebellar cortex in the rat. II. Phases in the maturation of Purkinje cells and of the molecular layer. *J Comp Neurol* 145:399–463. [CrossRef](#) [Medline](#)
- Altman J (1982) Morphological development of the rat cerebellum and some of its mechanism. *Exp Brain Res Suppl* 6:8–49.
- Amaral DG, Schumann CM, Nordahl CW (2008) Neuroanatomy of autism. *Trends Neurosci* 31:137–145. [CrossRef](#) [Medline](#)
- Apps R, Garwicz M (2005) Anatomical and physiological foundations of cerebellar information processing. *Nat Rev Neurosci* 6:297–311. [CrossRef](#) [Medline](#)
- Apps R, Hawkes R (2009) Cerebellar cortical organization: a one-map hypothesis. *Nat Rev Neurosci* 10:670–681. [CrossRef](#) [Medline](#)
- Ashwell K (1990) Microglia and cell death in the developing mouse cerebellum. *Dev Brain Res* 55:219–230. [Medline](#)
- Auger AP, Olesen KM (2009) Brain sex differences and the organization of juvenile social play behaviour. *J Neuroendocrinol* 21:519–525. [CrossRef](#) [Medline](#)
- Ayoub AE, Salm AK (2003) Increased morphological diversity of microglia in the activated hypothalamic supraoptic nucleus. *J Neurosci* 23:7759–7766. [Medline](#)
- Bauman ML, Kemper TL (2005) Neuroanatomic observations of the brain in autism: a review and future directions. *Int J Dev Neurosci* 23:183–187. [CrossRef](#) [Medline](#)
- Berbel P, Innocenti GM (1988) The development of the corpus callosum in cats: a light- and electron-microscopic study. *J Comp Neurol* 276:132–156. [CrossRef](#) [Medline](#)
- Burgoyne RD, Cambray-Deakin MA (1988) The cellular neurobiology of neuronal development: the cerebellar granule cell. *Brain Res* 472:77–101. [Medline](#)
- Butts T, Green MJ, Wingate RJ (2014) Development of the cerebellum: simple steps to make a “little brain”. *Development* 141:4031–4041. [CrossRef](#) [Medline](#)
- Carletti B, Rossi F (2008) Neurogenesis in the cerebellum. *Neuroscientist* 14:91–100. [CrossRef](#) [Medline](#)
- Cătălin B, Cupido A, Iancău M, Albu CV, Kirchhoff F (2013) Microglia: first responders in the central nervous system. *Rom J Morphol Embryol* 54:467–472. [Medline](#)
- Cuadros MA, Rodríguez-Ruiz J, Calvente R, Almendros A, Marín-Teva JL, Navascués J (1997) Microglia development in the quail cerebellum. *J Comp Neurol* 389:390–401. [Medline](#)
- D’Amelio M, Sheng M, Cecconi F (2012) Caspase-3 in the central nervous system: beyond apoptosis. *Trends Neurosci* 35:700–709.
- Dean SL, McCarthy MM (2008) Steroids, sex and the cerebellar cortex: implications for human disease. *Cerebellum* 7:38–47. [CrossRef](#) [Medline](#)
- Durisko C, Fiez JA (2010) Functional activation in the cerebellum during working memory and simple speech tasks. *Cortex* 46:896–906. [CrossRef](#) [Medline](#)
- Friauf E (1992) Tonotopic order in the adult and developing auditory system of the rat as shown by c-fos immunocytochemistry. *Eur J Neurosci* 4:798–812. [Medline](#)
- Glickstein M (1992) The cerebellum and motor learning. *Curr Opin Neurobiol* 2:802–806. [Medline](#)
- Glickstein M, Strata P, Voogd J (2009) Cerebellum: history. *Neuroscience* 162:549–559. [CrossRef](#) [Medline](#)
- Goldowitz D, Hamre K (1998) The cells and molecules that make a cerebellum. *Trends Neurosci* 21:375–382. [Medline](#)
- Gómez-Gonzalez B, Escobar A (2010) Prenatal stress alters microglial development and distribution in postnatal rat brain. *Acta Neuropathol* 119:303–315. [CrossRef](#) [Medline](#)
- Gottwald B, Mihajlovic Z, Wilde B, Mehdorn HM (2003) Does the cerebellum contribute to specific aspects of attention? *Neuropsychologia* 41:1452–1460. [Medline](#)
- Haraguchi S, Sasahara K, Shikimi H, Honda S, Harada N, Tsutsui K (2012) Estradiol promotes purkinje dendritic growth, spinogenesis, and synaptogenesis during neonatal life by inducing the expression of BDNF. *Cerebellum* 11:416–417. [CrossRef](#) [Medline](#)
- Hashimoto K, Kano M (2005) Postnatal development and synapse elimination of climbing fiber to Purkinje cell projection in the cerebellum. *Neurosci Res* 53:221–228. [CrossRef](#) [Medline](#)
- Heinsen H (1977) Quantitative anatomical studies on the postnatal development of the cerebellum of the albino rat. *Anat Embryol (Berl)* 151:201–218. [Medline](#)
- Holstege G, Georgiadis JR, Paans AM, Meiners LC, van der Graaf FH, Reinders AA (2003) Brain activation during human male ejaculation. *J Neurosci* 23:9185–9193. [Medline](#)
- Hyman BT, Yuan J (2012) Apoptotic and non-apoptotic roles of caspases in neuronal physiology and pathophysiology. *Nat Rev Neurosci* 13:395–406. [CrossRef](#) [Medline](#)
- Ito D, Imai Y, Ohsawa K, Nakajima K, Fukuchi Y, Kohsaka S (1998) Microglia-specific localisation of a novel calcium binding protein, Iba1. *Brain Res Mol Brain Res* 57:1–9. [Medline](#)
- Kaur C, Sivakumar V, Zou Z, Ling EA (2014) Microglia-derived pro-inflammatory cytokines tumor necrosis factor-alpha and interleukin-1beta induce Purkinje neuronal apoptosis via their receptors in hypoxic neonatal rat brain. *Brain Struct Funct* 219:151–170. [CrossRef](#) [Medline](#)
- Lenz KM, Nugent BM, Haliyur R, McCarthy MM (2013) Microglia are essential to masculinization of brain and behavior. *J Neurosci* 33:2761–2772. [CrossRef](#) [Medline](#)
- Lossi L, Mioletti S, Merighi A (2002) Synapse-independent and synapse-dependent apoptosis of cerebellar granule cells in postnatal rabbits occur at two subsequent but partly overlapping developmental stages. *Neuroscience* 112:509–523. [Medline](#)
- Marín-Teva JL, Dusart I, Colin C, Gervais A, van Rooijen N, Mallat M (2004) Microglia promote the death of developing Purkinje cells. *Neuron* 41:535–547. [Medline](#)
- McKay BE, Turner RW (2005) Physiological and morphological development of the rat cerebellar Purkinje cell. *J Physiol* 567:829–850. [CrossRef](#) [Medline](#)
- Meaney M, Stewart J (1981) A descriptive study of social development in the rat (*rattus norvegicus*). *Anim Behav* 29:34–45. [CrossRef](#)
- Miquel M, Toledo R, García LI, Coria-Avila GA, Manzo J (2009) Why should we keep the cerebellum in mind when thinking about addiction? *Curr Drug Abuse Rev* 2:26–40. [Medline](#)
- Moulton EA, Elman I, Becerra LR, Goldstein RZ, Borsook D (2014) The cerebellum and addiction: insights gained from neuroimaging research. *Addict Biol* 19:317–331. [Medline](#)
- Moulton EA, Schmähmann JD, Becerra L, Borsook D (2010) The cerebellum and pain: passive integrator or active participator? *Brain Res Rev* 65:14–27. [CrossRef](#) [Medline](#)
- Murdoch BE (2010) The cerebellum and language: historical perspective and review. *Cortex* 46:858–868. [CrossRef](#) [Medline](#)
- Nayak D, Roth TL, McGavern DB (2014) Microglia development and function. *Annu Rev Immunol* 32:367–402. [CrossRef](#) [Medline](#)
- Neumann H, Kotter MR, Franklin RJ (2009) Debris clearance by microglia: an essential link between degeneration and regeneration. *Brain* 132:288–295. [CrossRef](#) [Medline](#)
- Nimmerjahn A, Kirchhoff F, Helmchen F (2005) Resting microglial cells are highly dynamic surveillants of brain parenchyma in vivo. *Science* 308:1314–1318. [CrossRef](#) [Medline](#)
- Oomman S, Finckbone V, Dertien J, Attridge J, Henne W, Medina M, Mansouri B, Singh H, Strahlendorf H, Strahlendorf J (2004) Active caspase-3 expression during postnatal development of rat cerebellum is not systematically or consistently associated with apoptosis. *J Comp Neurol* 476:154–173. [CrossRef](#) [Medline](#)
- Panksepp J (1981) The ontogeny of play in rats. *Dev Psychobiol* 14:327–332. [CrossRef](#) [Medline](#)

- Paolicelli RC, Bolasco G, Pagani F, Maggi L, Scianni M, Panzanelli P, Giustetto M, Ferreira TA, Guiducci E, Dumas L, Ragozzino D, Gross CT (2011) Synaptic pruning by microglia is necessary for normal brain development. *Science* 333:1456–1458. [CrossRef](#) [Medline](#)
- Parnaik R, Raff MC, Scholes J (2000) Differences between the clearance of apoptotic cells by professional and non-professional phagocytes. *Curr Biol* 10:857–860. [Medline](#)
- Perez-Pouchoulen M, Miquel M, Saft P, Brug B, Toledo R, Hernandez ME, Manzo J (2012) The cerebellum in Autism. *e-Neurobiologia* 3:1–11.
- Ransohoff RM, Perry VH (2009) Microglial physiology: unique stimuli, specialized responses. *Annu Rev Immunol* 27:119–145. [CrossRef](#) [Medline](#)
- Rapoport M, van Reekum R, Mayberg H (2000) The role of the cerebellum in cognition and behavior: a selective review. *J Neuropsychiatry Clin Neurosci* 12:193–198. [Medline](#)
- Reiter LW, Anderson GE, Laskey JW, Cahill DF (1975) Developmental and behavioral changes in the rat during chronic exposure to lead. *Environ Health Perspect* 12:119–123. [Medline](#)
- Saab CY, Willis WD (2003) The cerebellum: organization, functions and its role in nociception. *Brain Res Brain Res Rev* 42:85–95. [Medline](#)
- Sarna JR, Hawkes R (2003) Patterned Purkinje cell death in the cerebellum. *Prog Neurobiol* 70:473–507. [Medline](#)
- Schafer DP, Lehrman EK, Kautzman AG, Koyama R, Mardinly AR, Yamasaki R, Ransohoff RM, Greenberg ME, Barres BA, Stevens B (2012) Microglia sculpt postnatal neural circuits in an activity and complement-dependent manner. *Neuron* 74:691–705. [CrossRef](#) [Medline](#)
- Schwarz JM, Sholar PW, Bilbo SD (2012) Sex differences in microglial colonization of the developing rat brain. *J Neurochem* 120:948–963. [CrossRef](#) [Medline](#)
- Shalini S, Dorstyn L, Dawar S, Kumar S (2015) Old, new and emerging functions of caspases. *Cell Death Differ* 22:526–539. [CrossRef](#) [Medline](#)
- Sierra A, Abiega O, Shahraz A, Neumann H (2013) Janus-faced microglia: beneficial and detrimental consequences of microglial phagocytosis. *Front Cell Neurosci* 7:6. [CrossRef](#) [Medline](#)
- Sierra A, Encinas JM, Deudero JJ, Chancey JH, Enikolopov G, Overstreet-Wadiche LS, Tsirka SE, Maletic-Savatic M (2010) Microglia shape adult hippocampal neurogenesis through apoptosis-coupled phagocytosis. *Cell Stem Cell* 7:483–495. [CrossRef](#) [Medline](#)
- Sillitoe RV, Joyner AL (2007) Morphology, molecular codes, and circuitry produce the three-dimensional complexity of the cerebellum. *Annu Rev Cell Dev Biol* 23:549–577. [CrossRef](#) [Medline](#)
- Sotelo C (2004) Cellular and genetic regulation of the development of the cerebellar system. *Prog Neurobiol* 72:295–339. [CrossRef](#) [Medline](#)
- Strata P (2015) The emotional cerebellum. *Cerebellum*. Advance online publication. doi:10.1007/s12311-015-0649-9.
- Strick PL, Dum RP, Fiez JA (2009) Cerebellum and nonmotor function. *Annu Rev Neurosci* 32:413–434. [CrossRef](#) [Medline](#)
- Swanson JA (2008) Shaping cups into phagosomes and macropinosomes. *Nat Rev Mol Cell Biol* 9:639–649. [CrossRef](#) [Medline](#)
- Tanaka M (2009) Dendrite formation of cerebellar Purkinje cells. *Neurochem Res* 34:2078–2088. [CrossRef](#) [Medline](#)
- ten Donkelaar HJ, Lammens M, Wesseling P, Thijssen HO, Renier WO (2003) Development and developmental disorders of the human cerebellum. *J Neurol* 250:1025–1036. [CrossRef](#) [Medline](#)
- Tremblay ME, Lowery RL, Majewska AK (2010) Microglial interactions with synapses are modulated by visual experience. *PLoS Biol* 8:e1000527. [CrossRef](#) [Medline](#)
- Tremblay ME, Stevens B, Sierra A, Wake H, Bessis A, Nimmerjahn A (2011) The role of microglia in the healthy brain. *J Neurosci* 31:16064–16069. [CrossRef](#) [Medline](#)
- Vargas DL, Nascimbene C, Krishnan C, Zimmerman AW, Pardo CA (2005) Neuroglial activation and neuroinflammation in the brain of patients with autism. *Ann Neurol* 57:67–81. [CrossRef](#) [Medline](#)
- Vela JM, Dalmau I, González B, Castellano B (1995) Morphology and distribution of microglial cells in the young and adult mouse cerebellum. *J Comp Neurol* 361:602–616. [CrossRef](#) [Medline](#)
- Voogd J, Glickstein M (1998) The anatomy of the cerebellum. *Trends Neurosci* 21:370–375. [Medline](#)
- Werling DM, Geschwind DH (2013) Sex differences in autism spectrum disorders. *Curr Opin Neurol* 26:146–153. [CrossRef](#) [Medline](#)
- Williamson LL, Sholar PW, Mistry RS, Smith SH, Bilbo SD (2011) Microglia and memory: modulation by early-life infection. *J Neurosci* 31:15511–15521. [CrossRef](#) [Medline](#)
- Wood KA, Dipasquale B, Youle RJ (1993) In situ labeling of granule cells for apoptosis-associated DNA fragmentation reveals different mechanisms of cell loss in developing cerebellum. *Neuron* 11:621–632. [Medline](#)
- Wu CH, Wen CY, Shieh JY, Ling EA (1992) A quantitative and morphometric study of the transformation of amoeboid microglia into ramified microglia in the developing corpus callosum in rats. *J Anat* 181:423–430.